Bulletin of Mathematical Biology (2008) 70: 1326–1347
DOI 10.1007/s11538-008-9301-x

ORIGINAL ARTICLE

A Model for Mechano-Electrical Feedback Effects on Atrial Flutter Interval Variability

Michela Masé[a,*], Leon Glass[b], Flavia Ravelli[c]

[a] *Department of Physics, University of Trento, via Sommarive, 14, 38050 Povo, Trento, Italy*
[b] *Centre for Nonlinear Dynamics, Department of Physiology, McGill University, 3655 Prom. Sir William Osler, Montreal, Québec, Canada H3G1Y6*
[c] *Department of Physics, University of Trento, and Fondazione Bruno Kessler, via Sommarive, 14, 38050 Povo, Trento, Italy*

Received: 12 July 2007 / Accepted: 18 December 2007 / Published online: 18 March 2008

Abstract Atrial flutter is a supraventricular arrhythmia, based on a reentrant mechanism mainly confined to the right atrium. Although atrial flutter is considered a regular rhythm, the atrial flutter interval (i.e., the time interval between consecutive atrial activation times) presents a spontaneous beat-to-beat variability, which has been suggested to be related to ventricular contraction and respiration by mechano-electrical feedback. This paper introduces a model to predict atrial activity during atrial flutter, based on the assumption that atrial flutter variability is related to the phase of the reentrant activity in the ventricular and respiratory cycles. Thus, atrial intervals are given as a superimposition of phase-dependent ventricular and respiratory modulations. The model includes a simplified atrioventricular (AV) branch with constant refractoriness and conduction times, which allows the prediction of ventricular activations in a closed-loop with atrial activations. Model predictions are quantitatively compared with real activation series recorded in 12 patients with atrial flutter. The model predicts the time course of both atrial and ventricular time series with a high beat-to-beat agreement, reproducing $96 \pm 8\%$ and $86 \pm 21\%$ of atrial and ventricular variability, respectively. The model also predicts the existence of phase-locking of atrial flutter intervals during periodic ventricular pacing and such results are observed in patients. These results constitute evidence in favor of mechano-electrical feedback as a major source of cycle length variability during atrial flutter.

Keywords Atrial flutter · Supraventricular arrhythmias · Reentrant activity · Interval variability · Mathematical model · Phase-locking dynamics · Mechano-electrical feedback

*Corresponding author.
E-mail address: mase@science.unitn.it (Michela Masé).

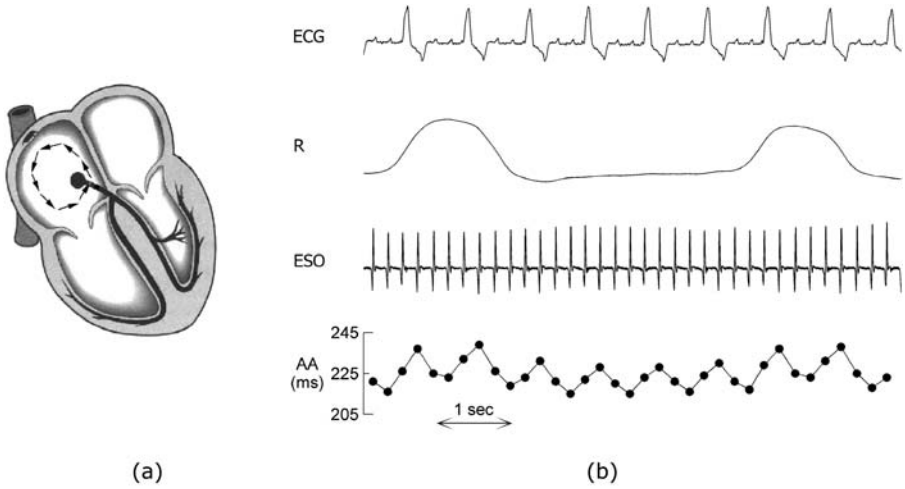

Fig. 1 (a) Schematic representation of the anatomical reentrant circuit responsible for atrial flutter. (b) Simultaneous recording of electrocardiogram (ECG), respiratory signal (R) and atrial electrogram (ESO) during atrial flutter and extraction of atrial flutter interval variability series (*AA*) from the atrial electrogram. *AA* intervals represent time intervals between consecutive activation times in the atrial electrogram.

1. Introduction

Atrial flutter is a supraventricular arrhythmia, based on a reentrant mechanism mainly confined to the right atrium (see Fig. 1(a), Waldo, 2000). The reentrant activity causes a very rapid (240–300 ms) and regular activation of the atria and the presence of some degree of atrioventricular (AV) block (mainly 2:1 and 4:1 ratios) due to the filtering action of the AV node.

Although atrial flutter is considered a regular rhythm, especially in comparison with atrial fibrillation, the atrial interval (i.e., the time interval between consecutive atrial activations indicated by *AA*) exhibits small beat-to-beat variations (see Fig. 1(b), bottom trace). This spontaneous variability is correlated to ventricular contraction (Lammers et al., 1991; Ravelli et al., 1994) and respiration (Waxman et al., 1991). Lammers et al. (1991) observed that the prolongation of the atrial flutter interval coincided with the increase of atrial volume following the ventricular ejection phase. Similarly, analyzing the effects of respiration, Waxman et al. (1991) observed the presence of longer *AA* intervals during inspiration, when an increased atrial stretch is observed due to the increase of the venous return to the heart. Both ventricular and respiratory atrial flutter interval oscillations were independent of autonomic tone (Waxman et al., 1991; Ravelli, 1998).

The hypothesis formulated to explain both these correlations belongs to the general framework of mechano-electrical feedback (Lab, 1982; Franz, 1996; Kohl and Ravens, 2003; Ravelli, 2003). Mechano-electrical feedback is the process by which changes in the mechanical state of cardiac tissue produce changes in its electrical behavior. Since both ventricular and respiratory activities involve cyclical modulations of atrial volume (Robotham et al., 1978; Matsuda et al., 1983), the fast reentrant electrical activity of the atria

during atrial flutter occurs at different degrees of atrial stretch and thus, through mechano-electrical feedback, in different geometrical and electrophysiological conditions. Therefore, ventricular and respiratory activities can affect atrial flutter intervals by a cyclical modulation of the anatomical and electrophysiological substrate of the atrial flutter reentrant circuit.

Based on the hypothesis that atrial flutter variability is associated to ventricular and respiratory activities through mechano-electrical feedback, the present paper aims to develop a mathematical model of atrial flutter interval variability. The model is conceived in "closed-loop," since ventricular activity, inducing modulation of atrial intervals, is predicted from atrial activity by including the basic properties of AV conduction. Respiration is regarded as an exogenous input to the model. The closed-loop model is validated by a quantitative comparison of predicted and real time series obtained in atrial flutter patients during basal condition. Predictions of the dynamical changes in atrial variability due to periodic forcing at different frequencies are obtained from the model and compared with data from patients under ventricular pacing and controlled respiration.

2. Data recording and time series extraction

In order to study the variability of atrial flutter interval due to ventricular contraction and respiration, atrial, ventricular, and respiratory activities were recorded in 12 patients with typical atrial flutter during an electrophysiological study. 10 patients (1–10) presented spontaneous 2:1 or 4:1 AV conduction block, while 2 patients (11–12) had been previously implanted with a permanent, programmable pacemaker, which allowed ventricular pacing at different frequencies. Atrial electrical activity was recorded by a bipolar catheter (interelectrode distance 2.2 cm) inserted into the esophagus (bandpass of 30–500 Hz). To monitor ventricular electrical activity, a body surface ECG was recorded simultaneously with the atrial electrogram and digitalized at 1 kHz. The nasal respiratory flow signal was recorded by a pressure transducer during spontaneous breathing and during controlled respiration at 0.2, 0.3 and 0.4 Hz. An example of the recorded signals is shown in Fig. 1(b). The study was approved by the local ethical committee and all patients gave written informed consent.

Data files were analyzed in series of 60 seconds in each patient. In four patients, longer time series (two to three minutes) were acquired to test the temporal stability of the model. Time series were automatically extracted from the recorded signals and manually checked and corrected. To extract atrial activation times, atrial electrograms were bandpass filtered (40–250 Hz, order 40, Kaiser window) and the modulus of the filtered signal was further low-pass filtered (FIR, 20 Hz, order 40, Kaiser window) (Botteron and Smith, 1995). Atrial depolarizations corresponded to the peaks of the filtered signal, which were larger than an adaptive threshold. For each detected depolarization, the activation time was the time of maximal, positive slope of the signal. The regular shape of the atrial waveform during atrial flutter allowed a high precision (within ± 1 ms error) in the estimation of activation times. Ventricular activation times were measured from the ECG by identifying the time of QRS maxima/minima, depending on the lead. Atrial (*AA*) and ventricular (*VV*) intervals were obtained as intervals between consecutive atrial and ventricular activation time series, respectively. The maxima of the respiratory signal were chosen as reference events for respiratory activity.

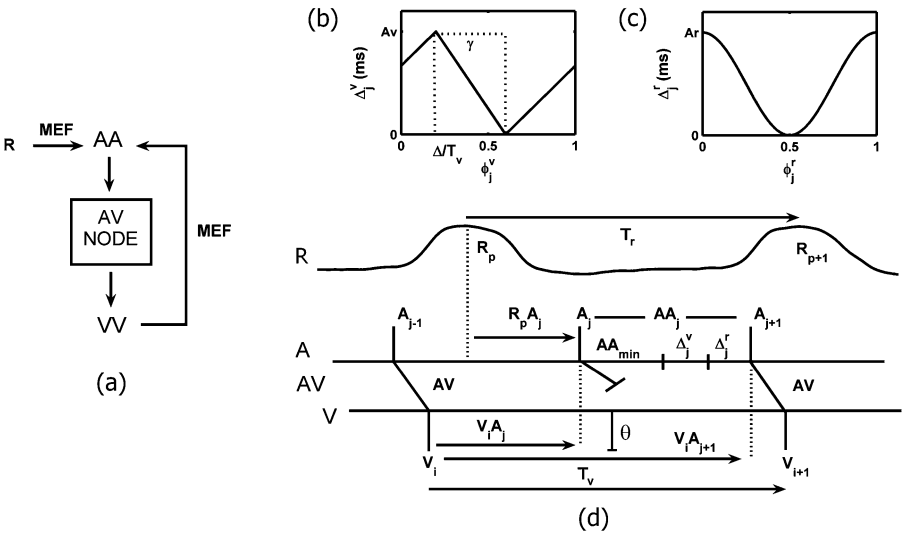

Fig. 2 (a) Electrophysiological principles of the model. Atrial activation determines ventricular activation after being filtered by the atrioventricular (AV) node. In turn, ventricular contraction and respiration modulate atrial activity through mechano-electrical feedback (MEF). (b) and (c) Functional dependence of ventricular Δ_j^v and respiratory Δ_j^r modulations on the ventricular $\phi_j^v = V_i A_j / T_v$ and respiratory $\phi_j^r = R_p A_j / T_r$ phases of the atrial intervals in the ventricular and respiratory cycles. (d) Schematic representation of the mathematical model. An atrial input impinging the AV node at time A_{j-1} is conducted to the ventricle with a nodal conduction time *AV*, which leads to a ventricular beat at time V_i. In turn, the ventricular beat V_i and the respiratory event R_p produce the phase-dependent modulations Δ_j^v and Δ_j^r on the duration of the following *AA* intervals, defining the occurrence of subsequent atrial beats. These are conducted to the ventricles if their recovery time $V_i A_j$ is longer than the nodal refractory period θ and blocked otherwise.

3. Mathematical model

3.1. Model definition

An iterative, closed-loop model was developed according to the mechano-electrical feedback (MEF) hypothesis to predict atrial (*AA*) and ventricular (*VV*) interval series during atrial flutter. As depicted in the schematic drawing in Fig. 2(a), we assume that atrial and ventricular activities interact in a closed-loop. Atrial activity determines ventricular activity after filtering by the AV node, while in turn ventricular activity modulates atrial activity by mechano-electrical feedback. In addition to the closed-loop structure, we assume that respiration (R) exerts an exogenous modulation on atrial activity by mechano-electrical feedback.

For the purpose of the following description, the model is conceptually divided into two parts, the MEF branch, which reproduces both ventricular and respiratory modulation effects on atrial flutter variability and the AV branch, which models the dynamics of the AV node.

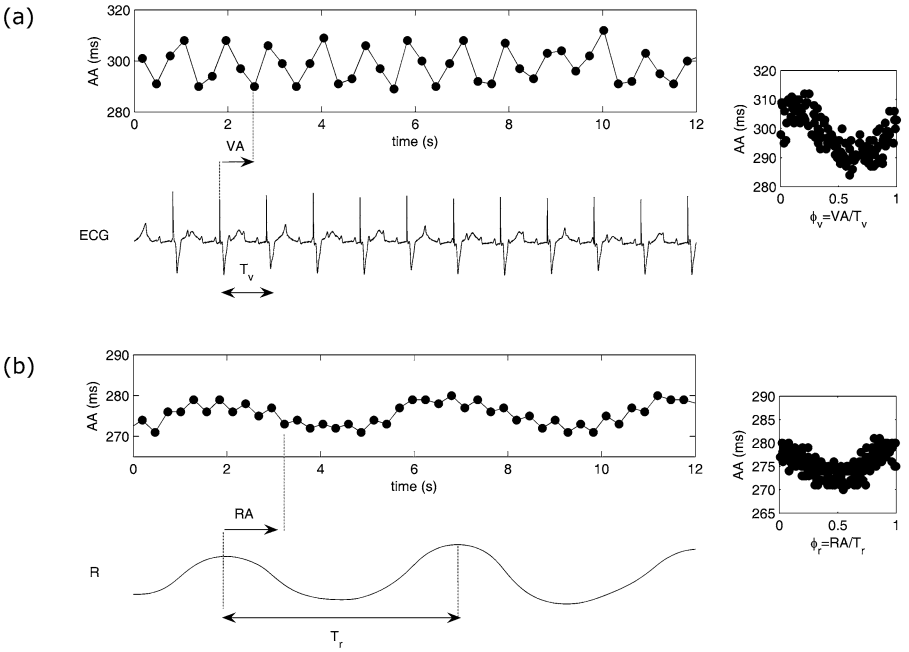

Fig. 3 Phase plots of atrial flutter intervals in ventricular and respiratory cycles. (a) Atrial interval time series *AA* (left, upper panel) and phase plot (right, upper panel) displayed with the corresponding ECG signal (lower panel) during periodic ventricular pacing at 1000 ms in patient 11. (b) Atrial interval time series *AA* (left, upper panel) and phase plot (right, upper panel) displayed with the corresponding respiratory signal (lower panel) during metronomic respiration at 0.2 Hz in patient 7. Phase plots evidence the presence of cyclical modulations in atrial variability correlated to ventricular contraction and respiration, since atrial intervals occurring at the same ventricular ϕ_j^v or respiratory ϕ_j^r phase assume similar values. Specifically, the ventricular phase plot shows atrial intervals to increase linearly to a maximal value following ventricular activation, and successively to decrease linearly to a minimal value. The respiratory phase plot shows a smooth decrease and successive increase of atrial intervals in respiratory cycle.

3.1.1. MEF branch of the model

Mechano-electrical feedback effects on *AA* variability are accounted for in the model by introducing a phase-dependent modulation on atrial intervals due to ventricular and respiratory effects.

If T_v is the period of ventricular activation and T_r is the period of respiration, we define for each atrial interval AA_j its phase ϕ_j^v in the ventricular cycle as:

$$\phi_j^v = \frac{V_i A_j}{T_v}, \quad 0 \le \phi_j^v \le 1 \tag{1}$$

and its phase ϕ_j^r in the respiratory cycle as:

$$\phi_j^r = \frac{R_p A_j}{T_r}, \quad 0 \le \phi_j^r \le 1, \tag{2}$$

where $V_i A_j$ and $R_p A_j$ are the time intervals between the jth atrial activation time and the previous closest ventricular beat V_i (refer to Fig. 3(a), left panel) and respiratory event R_p (refer to Fig. 3(b), left panel), respectively.

Successive atrial activation times are calculated, defining atrial intervals as the sum of three terms (see Fig. 2(d)):

$$AA_j = AA_{\min} + \Delta_j^v + \Delta_j^r, \tag{3}$$

where $AA_{\min}$ is a constant value and Δ_j^v and Δ_j^r are the ventricular and respiratory modulations, respectively.

Referring to the phase dependence relation in recorded data (Fig. 3(a), right panel), we assume that the ventricular modulation Δ_j^v depends on the phase ϕ_j^v of atrial intervals in the ventricular cycle, according to the piecewise linear function:

$$\Delta_j^v = \begin{cases} A_v + \frac{A_v}{1-\gamma}\left(\phi_j^v - \frac{\Delta}{T_v}\right), & 0 \le \phi_j^v \le \frac{\Delta}{T_v}, \\ A_v + \frac{A_v}{\gamma}\left(-\phi_j^v + \frac{\Delta}{T_v}\right), & \frac{\Delta}{T_v} \le \phi_j^v \le \frac{\Delta}{T_v} + \gamma, \\ \frac{A_v}{1-\gamma}\left(\phi_j^v - \frac{\Delta}{T_v} - \gamma\right), & \frac{\Delta}{T_v} + \gamma \le \phi_j^v \le 1, \end{cases} \tag{4}$$

where A_v is the maximal amplitude of ventricular modulation, $\frac{\Delta}{T_v}$ and γ are, respectively, the phase shift and the duration of the decreasing part of the triangular modulation (Fig. 2(b)).

In analogy, referring to the phase dependence relation in recorded data (Fig. 3(b), right panel), we assume that the respiratory modulation Δ_j^r depends on the phase ϕ_j^r of atrial intervals in respiratory cycle, according to the harmonic function:

$$\Delta_j^r = \frac{A_r}{2}\left(1 + \cos\left(2\pi\phi_j^r\right)\right), \tag{5}$$

where A_r is the maximal amplitude of respiratory modulation (Fig. 2(c)).

3.1.2. AV branch of the model

The AV branch of the model is used to compute the timing of ventricular activations for given atrial inputs. This is accomplished by including the refractory and conductive properties of the AV node. Since after the conduction of an atrial impulse the AV node is refractory (i.e. it could not conduct other beats) for a time period θ, we assume that atrial impulses occurring before the end of the refractory period (i.e., beats having a recovery time $V_i A_j < \theta$) are blocked, while atrial impulses occurring after the refractory period (i.e., $V_i A_j \ge \theta$) are successfully conducted to the ventricles, leading to a ventricular activation after a conduction time AV. We assume constant refractory periods θ and conduction times AV, so that:

$$V_i A_j = \sum_{m=k}^{j-1} AA_m - AV, \tag{6}$$

where the AA_m are the modulated atrial intervals calculated according to Eq. (3) and k is the most recently conducted atrial beat.

A schematic representation of the model is depicted in Fig. 2(d). Once the parameters of the model are set, starting from a conducted beat and a series of respiratory events, the MEF branch of the model predicts successive atrial activation times by adding to the initial atrial event modulated *AA* intervals (Eq. (3)), which depend on the time of the atrial events with respect to previous ventricular (Eq. (4)) and respiratory events (Eq. (5)). The timing of successive atrial events is used in turn by the AV branch of the model to compute ventricular activation times (Eq. (6)). These are used by the MEF branch to compute ventricular modulations to atrial intervals, closing the loop structure of the model. Successive atrial and ventricular activation times are determined by iteration of the closed-loop procedure.

3.2. Model assessment and parameter estimation

In order to validate the mathematical model, sequences of computed *AA* and *VV* interval series were quantitatively compared with the corresponding series recorded in patients.

The beat-to-beat agreement between model and data series was estimated by calculation of the average distance D between the series (Jorgensen et al., 2002). To calculate D, the series were resampled at the same equidistantly spaced times $t_i = t_{i-1} + \Delta t$, with Δt chosen as $1/10$ of the minimal value of the series. The absolute value of the difference between real and predicted series was calculated for each t_i and the average distance D on all t_i was adopted as measure of beat-to-beat similarity. The calculation was performed for both atrial and ventricular cases on the 60 s time series leading to the atrial (D_{AA}) and ventricular distance (D_{VV}), respectively.

The minimization of the average distance D_{AA} over the parameter space was used as criterion to identify in each patient the set of parameters in the model, which produced the best agreement with real data.

3.3. Statistical analysis

Real and simulated *AA* and *VV* interval series were characterized by mean value, standard deviations (std) and range (i.e., difference between maximal and minimal value of the series). For data in which two variables were compared, the paired t-test was performed and a significance level of $p < 0.05$ was taken to represent statistical significance. MATLAB 7.0.1 (Mathworks, USA) software was used for the statistical analysis and to run the simulations.

4. Results

4.1. Validation of the complete mathematical model in basal condition

The accuracy of the model was tested in 10 patients with atrial flutter and 2:1 or 4:1 AV block.

4.1.1. Sensitivity analysis

A sensitivity analysis was performed to study the dependence of the model on MEF and *AV* parameters respectively. The results of the analysis performed in representative patient 10, with 4:1 AV block, are displayed in Figs. 4–5.

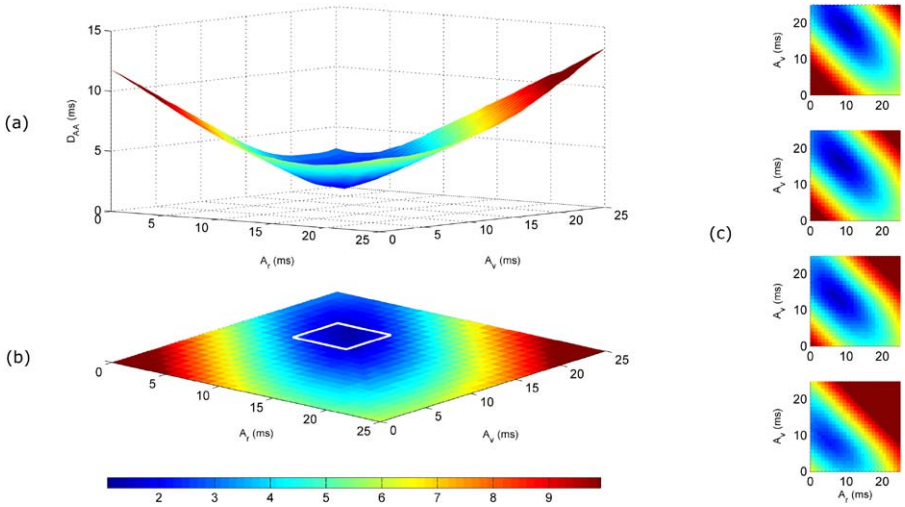

Fig. 4 Sensitivity analysis of the MEF branch of the model performed in patient 10. The dependence of the atrial distance D_{AA} on parameters A_v and A_r is displayed as a 3D surface plot (a) and graded color scale projection (b). D_{AA} values were calculated with fixed $\Delta = 230$ ms and $AA_{\min} = 216$ ms and using recorded ventricular and respiratory series as the input to the model. White lines enclose the region around the best parameter set, used as search space in the fit of the complete model. (c) Graded color scale projection of D_{AA} as function of (A_v, A_r) at changing $AA_{\min}$ values ($AA_{\min} = 214$ ms, 216 ms, 218 ms, 222 ms from top to bottom).

The sensitivity on MEF parameters was assessed by running the MEF branch of the model with real ventricular and respiratory series and characterizing the changes in the atrial distance D_{AA} at varying A_v, A_r and $AA_{\min}$. The values of D_{AA} define a smooth surface (Fig. 4(a)) with a single and well defined minimal region, when A_v and A_r are varied in the range 0–25 ms and $AA_{\min}$ is fixed to 216 ms. There is close agreement ($D_{AA} < 1.5$ ms) between data and model for (A_v, A_r) parameter combinations in the elliptic dark blue region (Fig. 4(b)). Projected (A_v, A_r) surfaces obtained for different $AA_{\min}$ values (Fig. 4(c)) show the elliptic dark blue region to move down-left (i.e., toward lower values of A_v and A_r) at increasing $AA_{\min}$. The region is present for 213 ms $\leq AA_{\min} \leq 219$ ms, thus in proximity of the minimum of the recorded AA series (217 ms). However, it progressively shrinks departing from $AA_{\min} = 216$ ms, where the minimum $D_{AA} = 1.19$ ms is observed.

The sensitivity of the model to AV parameters was assessed by running the AV branch of the model with real atrial series and characterizing the changes in the ventricular distance D_{VV} at varying AV and θ. The values of D_{VV}, corresponding to AV and θ varying in the range 0–1000 ms, describe a step-shaped surface (Fig. 5(a)), with $D_{VV} < 10$ ms in a diagonal strip region of the (AV, θ) parameter space. The presence of different (AV, θ) combinations resulting in good agreement between data and model is a consequence of the regularity of atrial activation during atrial flutter. Indeed, couples in the four different zones, indicated by numbers from 1 to 4 in Fig. 5(b), are consistent with the repeated transmission of one of the four atrial beat in each ventricular cycle, as schematized in Fig. 5(c). For instance, long refractory periods and short conduction times are associated

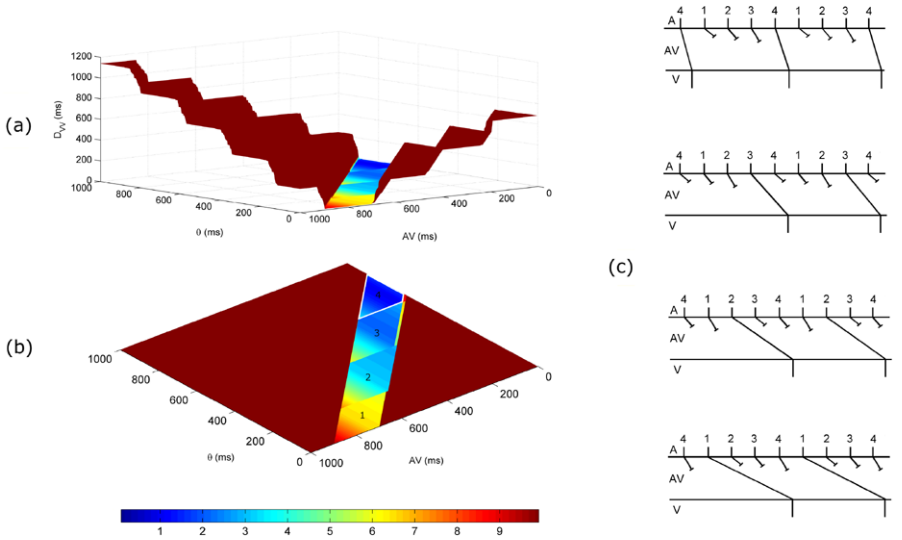

Fig. 5 Sensitivity analysis of the AV branch of the model performed in patient 10. The dependence of the ventricular distance D_{VV} on parameters AV and θ is displayed as a 3D surface plot (a) and color scale projection (b). D_{VV} values were calculated using recorded atrial series as the input to the model. White lines enclose the region around the best parameter set, used as search space in the fit of the complete model. (c). Ladder diagrams of the four possible conduction schemes of atrial beats in 4:1 atrial flutter. From top to bottom, transmission of the fourth, third, second, and first atrial beat in each ventricular cycle, corresponding to areas 4, 3, 2, and 1, respectively, in panel (b).

with the transmission of the fourth atrial beat (first panel from the top), while, short refractory periods and long conduction times are associated with the transmission of the first atrial beat in each cycle (fourth panel from the top). (AV, θ) couples consistent with the transmission of the fourth beat in each cycle (zone 4) lead to smaller D_{VV} values ($D_{VV} < 3$ ms, with minimal $D_{VV} = 1.02$ ms) (Fig. 5(b)).

The information provided by the MEF and AV sensitivity analysis allows to identify in each patient sub-regions of the parameter space (see white lines in Figs. 4–5) of the complete model, where the search of the minimal distance D_{AA} is performed to identify the best parameter set.

4.1.2. Model predictions

The final results of the fitting procedure for two paradigmatic patients characterized by 2:1 and 4:1 AV conduction ratios are displayed in Fig. 6 (panel (a) and (b), respectively), where the time course of AA (upper panels) and VV (lower panels) interval series are shown. The comparison of recorded (filled circles) and predicted (empty circles) atrial series shows the ability of the complete model to accurately predict ($D_{AA} = 1.31$ ms and 1.25 ms in (a) and (b), respectively) the pattern of variability in atrial intervals. The atrial variability is composed by high frequency ventricular modulation and low frequency respiratory modulation, with AA intervals varying within 218.9 ± 4.7 ms (a) and 227.6 ± 5.9 ms (b).

In addition, through its AV branch, the model accurately predicts ($D_{VV} = 1.9$ and 2.1 ms in (a) and (b), respectively) the respiratory modulated ventricular intervals. The

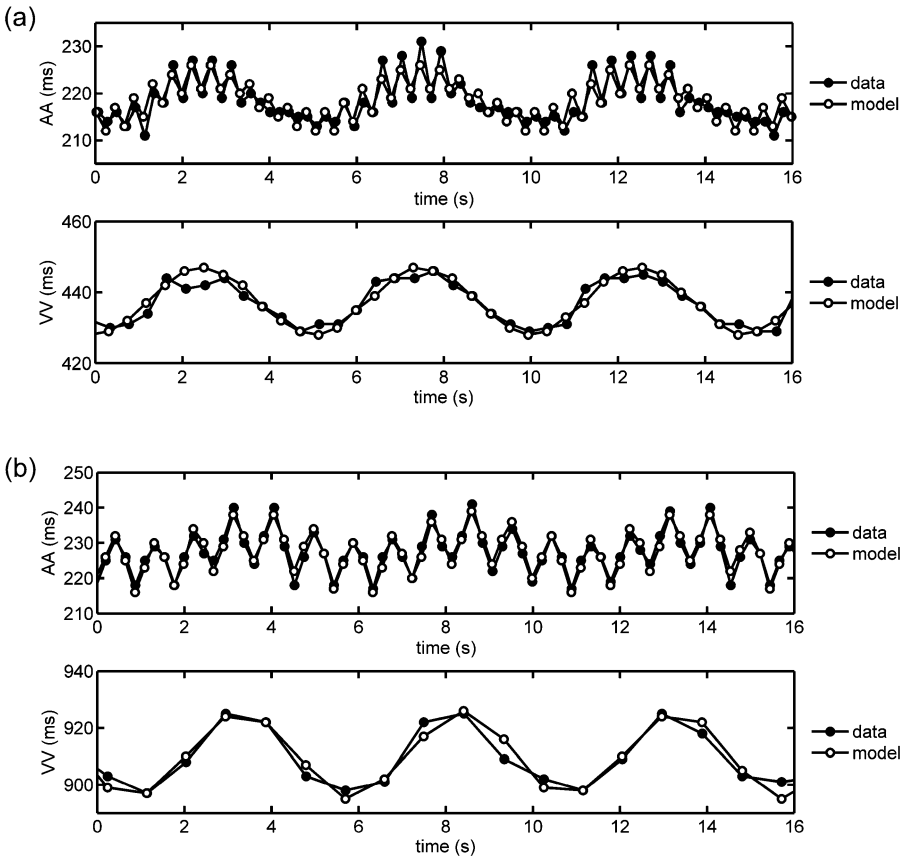

Fig. 6 Atrial *AA* and ventricular *VV* intervals from data and model in representative patient 6 with 2:1 (a) and patient 10 with 4:1 (b) AV blocks respectively. Simulated series were obtained by the complete model, setting $AA_{\min} = 211$ ms, $\Delta = 190$ ms, $A_v = 5.5$ ms, $A_r = 10.0$ ms, $AV = 68$ ms, $\theta = 268$ ms (a) and $AA_{\min} = 216$ ms, $\Delta = 230$ ms, $A_v = 16.0$ ms, $A_r = 8.0$ ms, $AV = 50$ ms, $\theta = 750$ ms (b).

amplitude of ventricular oscillations is of 22 ms (a) and 36 ms (b), with *VV* intervals varying within 438.0 ± 5.9 ms (a) and 910.6 ± 10.8 ms (b).

The good agreement between real and predicted time series is confirmed by the results of the analysis of the 60 s length series on the overall population of patients, summarized in Table 1. In fact, the model reproduces $96 \pm 8\%$ of atrial interval variability, with a mean distance D_{AA} between real and predicted time series of 1.1 ± 0.2 ms (corresponding to $9 \pm 2\%$ of *AA* range) and $86 \pm 21\%$ of ventricular interval variability, with a mean distance D_{VV} between predicted and real series of 3.2 ± 1.9 ms (corresponding to $11 \pm 3\%$ of *VV* range). In the four patients (6-7-8-10), where longer time series were acquired, model's predictions were carried out over longer times to test the temporal stability of the model. The results of the analysis show excellent agreement of the model with clinical data. The atrial series distances increase from $D_{AA} = 1.2 \pm 0.2$ ms to $D_{AA} = 1.5 \pm 0.1$ ms, when the number of points is increased from 250 ± 24 to 549 ± 163, while the ventricular series

Table 1 Observed and simulated mean and std of atrial *AA* and ventricular *VV* interval series in patients 1–10 with spontaneous AV block. Parameter sets corresponding to each simulation are indicated in the last column

Patient (AV block)		Data (ms)	Simulations (ms)	D (ms)	Parameter evaluation
1 (4:1)	*AA*	185.0 ± 1.8	185.0 ± 1.4	0.8	$AA_{\min} = 183$ ms, $\Delta = 130$ ms, $A_v = 4.0$ ms, $A_r = 0.0$ ms,
	VV	739.9 ± 2.4	740.0 ± 1.3	1.5	$AV = 285$ ms, $\theta = 277-477$ ms
2 (4:1)	*AA*	180.7 ± 7.4	180.6 ± 6.8	1.1	$AA_{\min} = 170$ ms, $\Delta = 0$ ms, $A_v = 21.5$ ms, $A_r = 0.5$ ms,
	VV	722.9 ± 4.1	722.3 ± 2.1	2.5	$AV = 298$ ms, $\theta = 258-398$ ms
3 (4:1)	*AA*	231.7 ± 6.1	231.7 ± 6.2	0.9	$AA_{\min} = 219$, $\Delta = 130$ ms, $A_v = 22.0$ ms, $A_r = 3.0$ ms,
	VV	928.0 ± 12.5	926.9 ± 4.0	5.8	$AV = 68$ ms, $\theta = 645-835$ ms
4 (4:1)	*AA*	192.6 ± 5.1	192.8 ± 5.0	0.9	$AA_{\min} = 183$ ms, $\Delta = 60$ ms, $A_v = 17.5$ ms, $A_r = 2.5$ ms,
	VV	770.3 ± 5.6	771.2 ± 3.7	4.1	$AV = 83$ ms, $\theta = 516-676$ ms
5 (2:1)	*AA*	235.5 ± 2.5	235.5 ± 1.7	1.2	$AA_{\min} = 233$ ms, $\Delta = 170$ ms, $A_v = 0.5$ ms, $A_r = 4.5$ ms,
	VV	471.1 ± 4.9	471.1 ± 3.2	2.2	$AV = 178$ ms, $\theta = 75-285$ ms
6 (2:1)	*AA*	218.9 ± 4.7	218.9 ± 3.9	1.3	$AA_{\min} = 211$ ms, $\Delta = 190$ ms, $A_v = 5.5$ ms, $A_r = 10.0$ ms,
	VV	438.0 ± 5.9	437.9 ± 7.3	1.9	$AV = 68$ ms, $\theta = 173-363$ ms
7 (2:1)	*AA*	275.4 ± 2.7	275.5 ± 2.5	0.9	$AA_{\min} = 270$, $\Delta = 240$ ms, $A_v = 5.0$, $A_r = 6.0$ ms,
	VV	550.8 ± 5.2	551.0 ± 4.1	2.1	$AV = 104$ ms, $\theta = 178-438$ ms
8 (2:1)	*AA*	289.3 ± 2.8	289.6 ± 2.4	1.1	$AA_{\min} = 282$ ms, $\Delta = 90$ ms, $A_v = 10.0$ ms, $A_r = 5.5$ ms,
	VV	578.6 ± 5.4	579.0 ± 4.0	3.1	$AV = 88$ ms, $\theta = 210-470$ ms
9 (4:1)	*AA*	224.6 ± 6.3	224.5 ± 6.1	1.4	$AA_{\min} = 212$ ms, $\Delta = 150$ ms, $A_v = 16.5$ ms, $A_r = 8.5$ ms,
	VV	898.1 ± 18.5	898.1 ± 11.0	7.1	$AV = 83$ ms, $\theta = 619-799$ ms
10 (4:1)	*AA*	227.6 ± 5.9	227.6 ± 5.8	1.3	$AA_{\min} = 216$ ms, $\Delta = 230$ ms, $A_v = 16.0$ ms, $A_r = 8.0$ ms,
	VV	910.6 ± 10.8	910.3 ± 10.8	2.1	$AV = 50$ ms, $\theta = 660-840$ ms

distances increase from $D_{VV} = 3.3 \pm 2.7$ ms to $D_{VV} = 3.8 \pm 2.6$ ms, when the number of points is increased from 92 ± 35 to 198 ± 68.

The best parameter set in each patient (Table 1, last column) provides a quantitative characterization of MEF effects and AV properties during atrial flutter. The estimation of MEF parameters shows a prevalent effect of ventricular contraction with respect to respiration in the determination of atrial flutter variability ($A_v = 11.9 \pm 7.8$ ms,

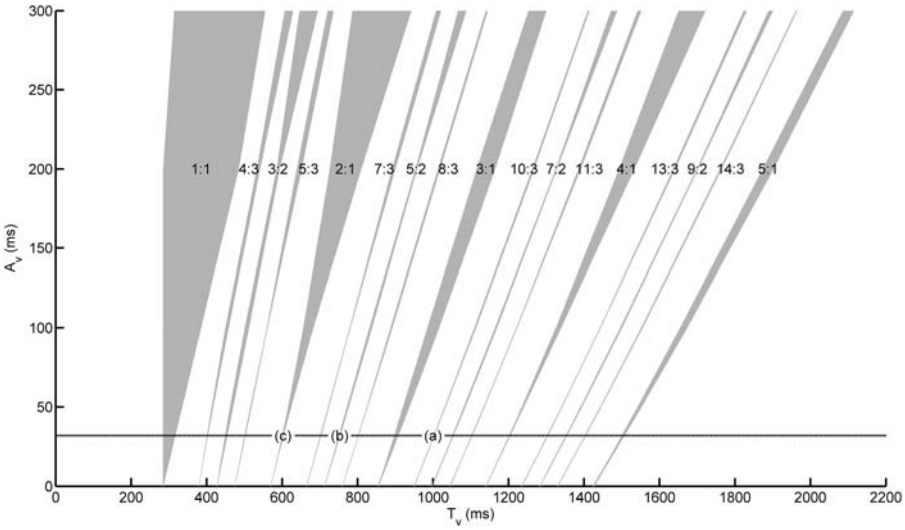

Fig. 7 Arnold tongues for the MEF ventricular branch of the model. Phase-locking regions up to depth $M = 3$ in a Farey series were numerically determined and indicated in gray. Simulations were run with parameters $AA_{\min} = 285$ ms, $\Delta = 150$ ms, $A_r = 0$ ms and varying 285 ms $\leq T_v \leq 2200$ ms (increment = 0.05 ms) and $A_v = [0\,10\,20\,30\,40\,50\,100\,200\,300]$. The dotted line indicates the estimated A_v value in patient 11. Letter (a), (b), (c) correspond to simulations in Fig. 8.

$A_r = 4.8 \pm 3.4$ ms, $p < 0.05$). With regard to AV conduction properties, longer refractory periods are observed in patients displaying 4:1 AV conduction compared to patients who displayed 2:1 AV conduction ($\theta = 583 \pm 115$ ms in 4:1 versus $\theta = 274 \pm 69$ ms in 2:1, $p < 0.05$). The large difference observed in refractory periods is commented in the discussion. No significant difference is observed in the conduction times ($AV = 145 \pm 115$ ms in 4:1 versus 110 ± 48 ms in 2:1, $p = 0.58$).

4.2. Periodic forcing of atrial flutter intervals

The effects of a periodic forcing on atrial flutter variability were studied by implementing the MEF ventricular branch of the model (Eqs. (3), (4)) and characterizing the patterns of atrial variability at different forcing period T_v and forcing amplitude A_v. Theoretical predictions were tested in the two patients (11–12) with programmable pacemakers.

As the stimulation period and amplitude are changed, periodic or quasiperiodic *AA* series are observed. The periodic rhythms consist of cycles containing N atrial intervals and M ventricular beats, which repeat with a period MT_v. This rhythm is called $N : M$ phase-locking rhythm, since atrial beats occurs at N different phases in the forcing ventricular cycle, and the fraction M/N is called phase-locking ratio.

The boundaries of the main ($M \leq 3$) phase-locking regions (called Arnold tongues (Arnold, 1991; Glass, 1991)) for the MEF ventricular branch of the model are sketched in Fig. 7. *AA* interval series are periodic for those sets of (T_v, A_v) values, which fall inside an Arnold tongue (indicated in gray), while parameter values outside the shown tongues correspond to higher order phase-locking or quasi-periodic dynamics. At increasing forcing

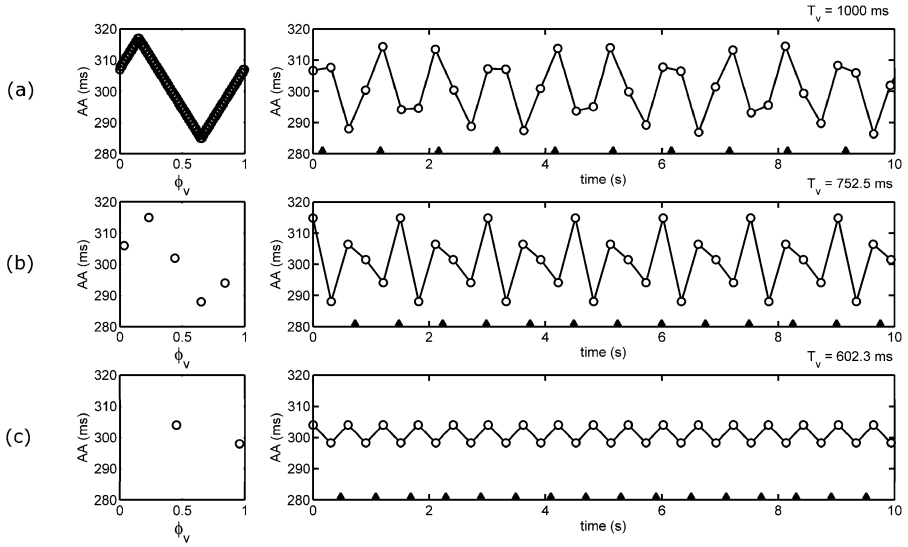

Fig. 8 Prediction of *AA* series variability during periodic forcing of atrial flutter intervals. Phase plots (left panels) and corresponding *AA* time series (right panels) obtained during periodic pacing at $T_v = 1000$ (a), 752.5 (b), and 602.3 (c) ms, indicated in Fig. 7. A quasi-periodic series is observed in (a), while 5:2 and 2:1 phase-locking are displayed in (b) and (c), respectively. Simulations were obtained by the MEF branch of the model, setting $AA_{\min} = 285$ ms, $\Delta = 150$ ms, $A_v = 32$ ms, $A_r = 0$ ms. Triangles at the bottom of each panel represent successive ventricular activation times.

period T_v, regions with decreasing phase-locking ratios are encountered. The sequence of the phase-locking ratio is ordered according to a typical Farey sequence (Allen, 1983; Bélair, 1986), since $(n + N) : (m + M)$ phase-locking regions are found between $n : m$ and $N : M$ regions.

The extension of the locking regions depends on the locking ratio and on the forcing amplitude A_v. For a given locking ratio, tongues get narrower at weaker modulation (i.e., smaller A_v), which indicates less chance of entrainment (i.e., phase-locking) of atrial variability in presence of weaker coupling. The physiological range for the modulation amplitude in atrial flutter patients was between 0.5 ms $\leq A_V \leq$ 33 ms and in the specific case of patient 11 and 12 the modulation amplitude was estimated in $A_v = 32$ ms (see dotted line) and 33 ms, respectively. Due to the weak modulation, low order phase-locking regions occupy a small area of the parameter space.

Predictions of atrial variability patterns in patient 11 are displayed in Fig. 8. An example of quasi-periodic pattern is observed at $T_v = 1000$ ms (Fig. 8(a)). In fact, the phase ϕ_v varies in subsequent ventricular cycles, covering all its 0–1 range. Consequently, the atrial intervals display large variability (std = 9.2 ms, range = 32 ms). Phase-locking regions present narrow extension. Specifically, the 2:1 phase-locking region is encountered for 600.40 ms $\leq T_v \leq$ 603.40 ms, while the 5:2 phase-locking region is observed for 750.60 ms $\leq T_v \leq$ 753.65 ms. Conditions of 5:2 and 2:1 phase-locking are exemplified in Fig. 8(b) and (c), respectively. Since the phase ϕ_v is bound to 5 and 2 values, respectively, the modulation curve is subsampled. In the 2:1 case, this results in a reduction of *AA* variability (std = 3.0 ms, range = 6.0 ms).

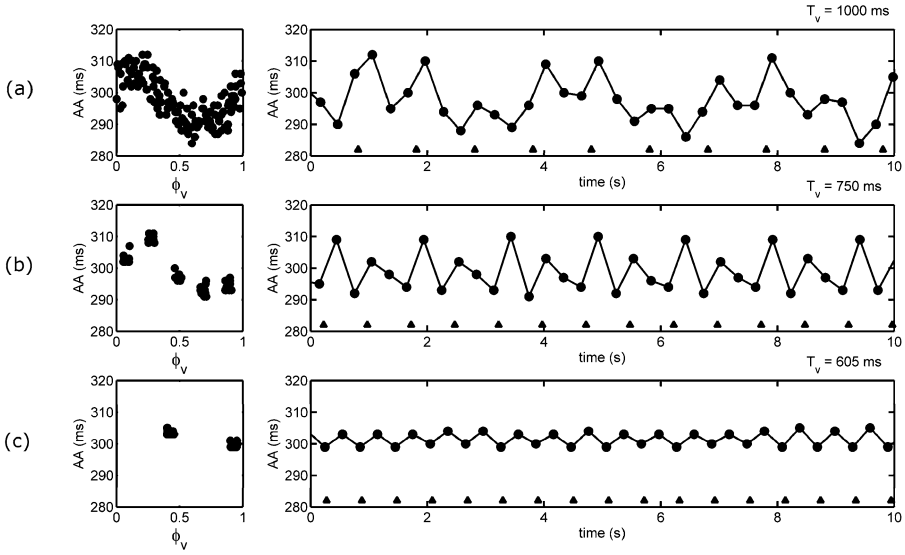

Fig. 9 *AA* series variability during periodic forcing by ventricular pacing in patient 11. Phase plots (left panels) and corresponding *AA* time series (right panels) obtained during pacing at period $T_v = 1000$ (a), 750 (b), and 605 (c) ms. 2:1 and 5:2 phase locking between atrial and ventricular activity in panels (b) and (c) correspond to the theoretical predictions of Fig. 8(b, c). Triangles at the bottom of each panel represent successive ventricular activation times.

Theoretical predictions were tested in the two patients with a permanent pacemaker by periodically pacing the ventricles during atrial flutter. In agreement with model predictions in patient 11 (Fig. 8(a)), there is no phase-locking for $T_v = 1000$ ms (Fig. 9(a)) and *AA* intervals display a high variability (std = 6.9 ms, range = 28 ms). In contrast, for pacing periods $T_v = 750$ ms (Fig. 9(b)) and $T_v = 605$ ms (Fig. 9(c)), close to the predicted 5:2 (Fig. 8(b)) and 2:1 (Fig. 8(c)) phase-locking regions, the phase results clusterized around 5 and 2 phase values, respectively, and periodic atrial series of 5:2 and 2:1 order are observed. In agreement with simulations, in the 2:1 case, the variability of the series decreases significantly (std = 2.1 ms, range = 6 ms). Theoretical predictions in patient 12 (with best parameter set $AA_{\min} = 270$ ms, $A_v = 33$ ms, $A_r = 0$ ms, $\Delta = 150$ ms) locate a 3:1 phase-locking region for ventricular pacing periods between 856.10 ms $\leq T_v \leq$ 859.05 ms. A 3:1 phase-locked atrial series is indeed observed during ventricular pacing at $T_v = 854$ ms.

A periodic forcing can be exerted on atrial flutter intervals also by controlling the MEF respiratory branch of the model. In this case, the patterns of atrial interval variability can be characterized at changing period of respiration T_r. Theoretical predictions obtained by the MEF part of the model were tested in three patients (6-7-10), where controlled respiration was performed at three different frequencies (i.e., 0.2, 0.3 and 0.4 Hz). Real and simulated *AA* series from representative patient 7 are displayed in Fig. 10. The decrease in the period of respiration from panel (a) to panel (c) results in an evident decrease in the period of oscillation of the envelope of atrial intervals. The model closely matches the observed data with small values of the distance $D_{AA} = 1.6 \pm 0.2$ ms. Similar results are obtained

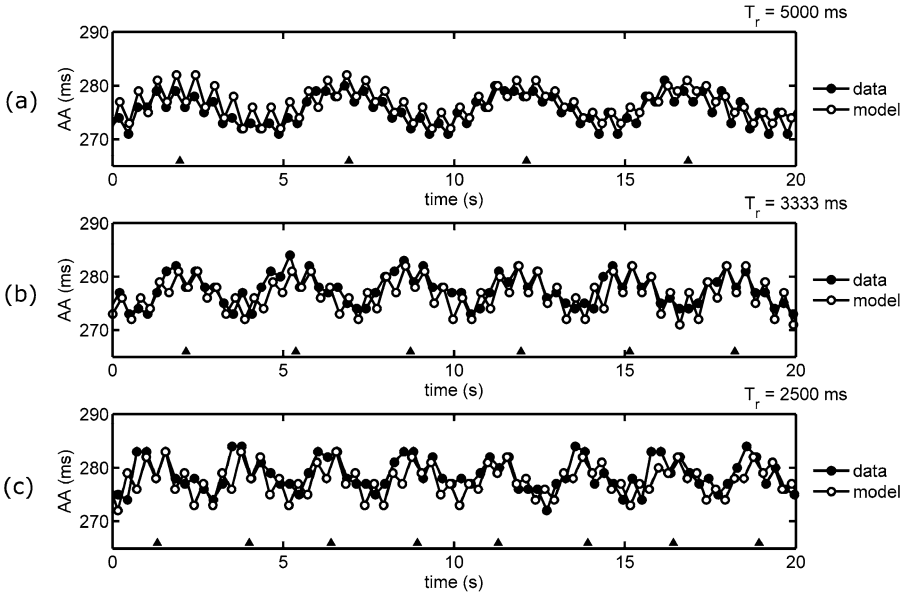

Fig. 10 *AA* series variability during periodic forcing by controlled respiration in patient 7. *AA* time series from data and model correspond to periodic breathing at $T_r = 5000$(a), 3333 (b), and 2500 (c) ms. Simulations were obtained by the MEF branch of the model, setting $AA_{\min} = 271$ ms, $\Delta = 190$ ms, $A_v = 5.5$ ms, $A_r = 6$ ms. Triangles at the bottom of each panel represent successive maxima of the respiratory signal.

in the two other patients, with agreement between model and data of $D_{AA} = 2.2 \pm 0.1$ ms and $D_{AA} = 1.7 \pm 0.3$ ms.

5. Discussion

In this work we developed a mathematical model of atrial flutter interval variability. The model is based on the MEF hypothesis that oscillations in *AA* intervals are produced by ventricular contraction and respiration (Lammers et al., 1991; Waxman et al., 1991; Ravelli et al., 1994), and thus it predicts *AA* series assuming interval perturbations dependent on the phases of the *AA* intervals in the ventricular and respiratory cycles. In addition, by including basic properties of AV conduction, the model is able to reproduce both atrial and ventricular time series in a closed-loop. Quantitative comparison of real data and model predictions showed the ability of the model to follow on a beat-to-beat basis the time course of both atrial ($D_{AA} = 1.1 \pm 0.2$ ms) and ventricular ($D_{VV} = 3.2 \pm 1.9$ ms) interval series, reproducing the most part of atrial and ventricular variability. Moreover simulations run by the MEF ventricular branch of the model at increasing ventricular pacing frequencies predicted the possibility to entrain atrial flutter variability by ventricular pacing. Periodic ventricular pacing of patients with atrial flutter led to entrainment similar to the theoretical predictions.

5.1. Mechano-electrical feedback hypothesis

Previous studies have shown the relationship between the atrial flutter interval and ventricular contraction (Lammers et al., 1991; Ravelli et al., 1994) and respiration (Waxman et al., 1991; Ravelli, 1998). This earlier work led to the development of the mechano-electrical feedback (MEF) hypothesis that changes in atrial volume directly affect atrial flutter variability, without mediation of the autonomic nervous system (Ravelli, 1998). Specifically, in mechano-electrical feedback general framework, the change in atrial volume and atrial stretch associated with ventricular cycle and respiration could modulate the revolution time of the reentry (and thus, the observed atrial flutter intervals) via a modulation of both geometric (i.e., circuit size) and electrophysiological factors.

Waxman et al. (1991) suggested that cardiac volume played a role in the determination of the atrial flutter interval, since they observed that the mean atrial flutter cycle length could be shortened by manoeuvres which decreased atrial volume, as passive upright tilting, the strain phase of the Valsalva manoeuvre and expiration. Correlation between atrial volume and mean atrial flutter period was observed also by Vulliemin et al. (1994), who stressed the importance of the right heart preload and atrial size for the electrophysiological characteristic of type I atrial flutter.

Experimental studies have demonstrated that stretch may modulate cardiac electrophysiological properties, such as action potential shape and duration (Lab, 1980; White et al., 1993; Riemer and Tung, 2003), tissue excitability (Tung and Zou, 1995; Riemer et al., 1998), passive and geometrical membrane properties (Deck, 1964; Dominguez and Fozzard, 1979), gap junction expression (Zhuang et al., 2000), and may provoke occurrence of ectopic activity (Franz, 1996). The modulation has been shown to operate on a beat-to-beat basis (Kaufmann et al., 1971; Lab, 1980, 1982) and to occur rapidly, involving a time lag of just 10–20 milliseconds (Kaufmann et al., 1971). Stretch-activated ion channels (Sachs, 1991; Hu and Sachs, 1997) and modulation of intracellular calcium concentration by stretch-enhanced myofilament Ca^{2+} sensitivity or by stretch-activated calcium influx (Calaghan and White, 1999) have been suggested as the most likely candidates in the process of transduction of membrane tension in electrophysiological changes.

Focusing on atrial tissue, experimental and clinical studies have shown that changes in mechanical loading conditions may affect macroscopic electrophysiological properties of the atrium (Nazir and Lab, 1996a; Franz and Bode, 2003; Ravelli, 2003). The major part of the studies in the atria has considered the effects of stretch on atrial refractoriness. While in vivo studies provided divergent results due to the variety of loading conditions and neurohumoral influences (Ravelli, 2003), experimental studies in isolated preparations clearly showed that atrial refractory period (Ravelli and Allessie, 1997; Bode et al., 2000; Zarse et al., 2001; Ninio et al., 2005) and action potential duration at early levels of repolarization (Nazir and Lab, 1996b; Tavi et al., 1998; Kamkin et al., 2000) were shortened by acute atrial dilatation. As concerns the effects of acute atrial dilatation on conduction velocity, consistent results were obtained in the isolated rabbit heart. Specifically, high-density mapping studies by Chorro et al. (1998) showed a global decrease of conduction velocity of about 25% in the right atrium by balloon inflation, while Eijsbouts et al. (2003) showed that acute atrial dilatation not only depressed atrial conduction, but also promoted spatial heterogeneity in conduction by causing conduction blocks.

Since the underlying mechanism of typical atrial flutter is a macro-reentry with large excitable gap (Waldo, 2000), the revolution time of the reentry should be determined

by its size and conduction velocity, while moderate changes in the refractory period are not expected to produce rate variations. Differently changes in the refractory period may have an influence on the rate of reentries around a functionally determined circuit, as in the case of the rapid form of atrial flutter (Ravelli et al., 1994). In the light of these considerations, the increase in atrial interval observed during both ventricular ejection phase and inspiration may be explained by the combination of stretch-induced slowing of conduction and lengthening of the reentrant pathway, which in turn determines an increase in the revolution time of the reentry and thus of the arrhythmia cycle length.

5.2. Mathematical model of MEF effects

This study presents a mathematical model of atrial flutter variability based on the MEF hypothesis formulated in previous studies. The model restricts the changes in mechanical environment to ventricular and respiratory inputs and schematizes these in terms of phase-dependent variability curves. This phenomenological approach allowed us to quantitatively demonstrate the plausibility of a mechanical modulation for atrial flutter variability, showing that during atrial flutter $96 \pm 8\%$ of atrial variability was associated to cyclical ventricular and respiratory modulations, with the former exerting the prevalent role.

The schematization of MEF effects in terms of phase-dependant variability curves allowed us to explain the dynamics of atrial flutter variability. Based on the development of the MEF ventricular branch of the model, we showed that atrial flutter variability could be influenced by periodic ventricular pacing. In particular simulations evidenced the possibility to entrain atrial flutter variability by ventricular pacing, yielding to phase-locking patterns of different orders. However, since physiologically reasonable values of the modulation amplitude produce narrow phase-locking regions, which occupy just a small portion of the parameter space, entrainment could be observed just for a small set of well-defined pacing periods. The ordering and structure of phase-locking regions is a consequence of the piecewise linear nature of the assumed modulation curve (i.e., Δ_j^v) and is consistent with previous works (Uherka et al., 1992; McGuinness et al., 2004). In fact, the modulation curve is associated with a piecewise linear circle map of the phase ϕ_j^v into itself. This map, of degree one, continuous on the circle and monotone increasing, is dynamically equivalent to the subcritical "tip maps" extensively studied by Uherka et al. (1992). Since these maps have well-defined rotation numbers, their possible behaviors are limited to quasi-periodicity and phase-locking, as indeed observed in our model.

5.3. AV branch of the model

Based on the development of an AV branch, our model predicts in a closed-loop the variability of ventricular interval during atrial flutter. The AV branch of our model, which adopts constant conduction times AV and refractory periods θ in each patient, is a simplification of previously proposed models of AV conduction, which assumed conduction times to depend on recovery times (Shrier et al., 1987) and/or refractory periods to be affected by concealed conduction (Jorgensen et al., 2002; Mangin et al., 2005), fatigue and facilitation (Heethaar et al., 1973; Billette and Nattel, 1994). The approximations adopted in our model are consistent with the characteristics of atrial activity during atrial flutter. In fact, the regularity of atrial activation implies almost fixed recovery times, and thus

fixed conduction times. On the other hand, fixed AV blocks involve almost constant contributions of concealed conduction on refractory periods, which justify the use of constant refractory periods.

Although the simplicity of the model, the AV parameters AV and θ provided a rough estimate of conduction and refractoriness during atrial flutter. The difference observed in the estimated refractory periods between patients with 2:1 and 4:1 conduction ratios is consistent with the concept of concealed conduction, which assumes that blocked beats have an effect on the conduction of successive beats (Langendorf, 1948). In particular, the longer refractory periods observed in 4:1 patient group (where 3 concealed beats per cycle are present) are in agreement with the experimental studies of Page et al. (1996), which showed that the main effect of concealed conduction was a consistent lengthening of the refractory period.

The ability of the model to predict with high beat-to-beat precision ventricular activation series demonstrated that respiratory mechanical modulations of atrial activity, filtered by the AV node, were responsible for most part ($86 \pm 21\%$) of ventricular variability during atrial flutter, while other factors as the autonomic nervous system (although known to affect both AV conduction (Warner et al., 1986; Warner and Loeb, 1986; Nollo et al., 1994; Kautzner et al., 2000) and concealed conduction effects (Page et al., 1996)) played a secondary role in heart rate variability during the arrhythmia.

6. Study limitations

The present model represents a phenomenological model of the variability of atrial and ventricular intervals during atrial flutter. Since no assumptions are made on the specific microscopic events leading to the lengthening of atrial intervals in presence of stretch, mechanistic aspects can not be reliably tested by the model. Ionic models of cardiac cells including stretch activated channels have been proposed (Sachs, 1994; Kohl et al., 1998; Rice et al., 1998; Riemer et al., 1998; Healy and McCulloch, 2005; Kuijpers et al., 2007), which incorporate linear, time independent, mechano-sensitive currents into single cell models, as well as one- and two-dimensional cardiac network models. These models quantitatively reproduce effects of maintained mechanical stretch on experimentally measured action potential characteristics such as amplitude, duration, maximum diastolic potential, peak upstroke velocity, and conduction velocity. However, their complexity hinders the actual reproduction of clinical data. By contrast, our mathematical model, reducing the cyclical changes in the mechanical environment to respiratory and ventricular inputs and reproducing the main aspects of AA variability by simplified rules, represents a complementary, rather than alternative, approach to the development of detailed ionic models. To bridge the gap between the two modeling perspectives, further studies should be performed aiming to clarify how changes in atrial stretch are translated into changes in the conduction properties of the reentrant circuit. These would involve beat-to-beat measurement of conduction velocity, refractory period and circuit pathway during atrial flutter, which are still a technical challenge in patients.

The model was tested on atrial and ventricular series of 60 s length. Longer series would be required to assess the long time predictions of the model and its possible drift from data over long iterations. Nevertheless, the application of the model in four of the

patients, where longer time series were available, shows excellent agreement of the model with clinical data over few minute recordings.

Since atrial flutter is nowadays typically treated by ablation therapy, the study of atrial flutter variability may not have a significant impact on the treatment of this arrhythmia. Nevertheless, as demonstrated by previous studies (Ravelli et al., 1994), the detailed analysis of the variations in cycle length can be used to study the underlying mechanism of atrial arrhythmias. The mechanical modulation of atrial flutter intervals has been used to elucidate the re-entrant mechanisms underlying different forms of atrial flutter (Ravelli et al., 1994). In addition, in selected categories of patients where antitachycardia pacing is the treatment of choice (Waldo, 2000), a better understanding of the anatomical and physiological basis of atrial flutter may lead to the development of better ways to terminate atrial flutter using optimal positioning of implantable antitachycardia devices and optimal timing of antitachycardia stimuli.

7. Conclusions

This work analyzed and modeled the spontaneous variability of atrial flutter. We hypothesized that due to mechano-electrical feedback, the variability was related to the phase of the reentrant activity in ventricular and respiratory cycles and thus we modeled the variability of atrial intervals in terms of phase-dependent ventricular and respiratory modulations. The closed-loop structure of the model, which included a simplified AV branch, allowed us to predict also the ventricular output, which induced the modulation of atrial activity. The quantitative comparison of real and predicted time series showed the ability of the model to predict atrial and ventricular activity on a beat-to-beat basis and allowed us to demonstrate that during atrial flutter $96 \pm 8\%$ and $86 \pm 21\%$ of atrial and ventricular variability, respectively, were mechanically-induced. Dynamical simulations run by the MEF ventricular branch of the model showed that atrial variability could be entrained by periodic, ventricular pacing and that well-defined patterns of variability arose at different pacing frequencies. These results constitute evidence in favor of mechano-electrical feedback as a major source of cycle length variability of atrial flutter.

Acknowledgements

Michela Masè is recipient of a fellowship supported by Fondazione Cassa di Risparmio di Trento e Rovereto. Leon Glass thanks the Canadian Heart and Stroke Foundation and the CIHR for financial support. The authors are very grateful to Dr. Marcello Disertori, Division of Cardiology, S. Chiara Hospital, Trento, Italy, for providing atrial flutter recordings.

References

Allen, T., 1983. On the arithmetic of phase locking: Coupled neurons as a lattice on R^2. Physica D 6(3), 305–320.

Arnold, V.I., 1991. Cardiac arrhythmias and circle mappings. Chaos 1(1), 20–24.

Bélair, J., 1986. Periodic pulsatile stimulation of a nonlinear oscillator. J. Math. Biol. 24(2), 217–232.

Billette, J., Nattel, S., 1994. Dynamic behavior of the atrioventricular node: a functional model of interaction between recovery, facilitation, and fatigue. J. Cardiovasc. Electrophysiol. 5(1), 90–102.

Bode, F., Katchman, A., Woosley, R.L., Franz, M.R., 2000. Gadolinium decreases stretch-induced vulnerability to atrial fibrillation. Circulation 101(18), 2200–2205.

Botteron, G.W., Smith, J.M., 1995. A technique for measurement of the extent of spatial organization of atrial activation during atrial fibrillation in the intact human heart. IEEE Trans. Biomed. Eng. 42(6), 579–586.

Calaghan, S.C., White, E., 1999. The role of calcium in the response of cardiac muscle to stretch. Prog. Biophys. Mol. Biol. 71(1), 59–90.

Chorro, F.J., Egea, S., Mainar, L., Canoves, J., Sanchis, J., Llavador, E., Lopez-Merino, V., Such, L., 1998. Acute changes in wavelength of the process of auricular activation induced by stretching. Experimental study. Rev. Esp. Cardiol. 51(11), 874–883.

Deck, K.A., 1964. Changes in the resting potential and the cable properties of Purkinje fibers during stretch. Pflugers Arch. Gesamte Physiol. Menschen. Tiere. 280, 131–140.

Dominguez, G., Fozzard, H.A., 1979. Effect of stretch on conduction velocity and cable properties of cardiac Purkinje fibers. Am. J. Physiol. 237(3), C119–C124.

Eijsbouts, S., Van Zandvoort, M., Schotten, U., Allessie, M., 2003. Effects of acute atrial dilation on heterogeneity in conduction in the isolated rabbit heart. J. Cardiovasc. Electrophysiol. 14(3), 269–278.

Franz, M.R., 1996. Mechano-electrical feedback in ventricular myocardium. Cardiovasc. Res. 32(1), 15–24.

Franz, M.R., Bode, F., 2003. Mechano-electrical feedback underlying arrhythmias: the atrial fibrillation case. Prog. Biophys. Mol. Biol. 82, 163–174.

Glass, L., 1991. Cardiac arrhythmias and circle maps-A classical problem. Chaos 1(1), 13–19.

Healy, S.N., McCulloch, A.D., 2005. An ionic model of stretch-activated and stretch-modulated currents in rabbit ventricular myocytes. Europace 7, 2128–2134.

Heethaar, R.M., Denier van der Gon, J.J., Meijler, F.L., 1973. Mathematical model of A-V conduction in the rat heart. Cardiovas. Res. 7(1), 105–114.

Hu, H., Sachs, F., 1997. Stretch-activated ion channels in the heart. J. Mol. Cell Cardiol. 29(6), 1511–1523.

Jorgensen, P., Schafer, C., Guerra, P.G., Talajic, M., Nattel, S., Glass, L., 2002. A mathematical model of human atrioventricular nodal function incorporating concealed conduction. Bull. Math. Biol. 64(6), 1083–1099.

Kamkin, A., Kiseleva, I., Wagner, K.D., Leiterer, K.P., Theres, H., Scholz, H., Gunther, J., Lab, M.J., 2000. Mechano-electric feedback in right atrium after left ventricular infarction in rats. J. Mol. Cell. Cardiol. 32(3), 465–477.

Kaufmann, R.L., Lab, M.J., Hennekes, R., Krause, H., 1971. Feedback interaction of mechanical and electrical events in the isolated mammalian ventricular myocardium (cat papillary muscle). Pflugers Arch. 324(2), 100–123.

Kautzner, J., Malik, M., Camm, A.J., 2000. Autonomic modulation of AV nodal conduction. In: Mazgalev, T.N., Tchou, P.J. (Eds.), Atrial-AV Nodal Electrophysiology: A view from the Millennium, pp. 237–250. Futura Publishing Company, New York

Kohl, P., Day, K., Noble, D., 1998. Cellular mechanisms of cardiac mechano-electric feedback in a mathematical model. Can. J. Cardiol. 14(1), 111–119.

Kohl, P., Ravens, U., 2003. Cardiac mechano-electric feedback: past, present, and prospect. Prog. Biophys. Mol. Biol. 82(1–3), 3–9.

Kuijpers, N.H., ten Eikelder, H.M., Bovendeerd, P.H., Verheule, S., Arts, T., Hilbers, P.A., 2007. Mechanoelectric feedback leads to conduction slowing and block in acutely dilated atria: a modeling study of cardiac electromechanics. Am. J. Physiol. Heart Circ. Physiol. 292(6), H2832–H2853.

Lab, M.J., 1980. Transient depolarisation and action potential alterations following mechanical changes in isolated myocardium. Cardiovas. Res. 14(11), 624–637.

Lab, M.J., 1982. Contraction-excitation feedback in myocardium. Physiological basis and clinical relevance. Circ. Res. 50(6), 757–766.

Lammers, W.J.E.P., Ravelli, F., Disertori, M., Antolini, R., Furlanello, F., Allessie, M.A., 1991. Variations in human atrial flutter cycle length induced by ventricular beats: evidence of a reentrant circuit with a partially excitable gap. J. Cardiovasc. Electrophysiol. 2(5), 375–387.

Langendorf, R., 1948. Concealed conduction: the effect of blocked impulses on the formation and conduction of subsequent impulses. Am. Heart J. 35, 542–552.

Mangin, L., Vinet, A., Page, P., Glass, L., 2005. Effects of antiarrhythmic drug therapy on atrioventricular nodal function during atrial fibrillation in humans. Europace 7, 271–282.

Matsuda, Y., Toma, Y., Ogawa, H., Matsuzaki, M., Katayama, K., Fujii, T., Yoshino, F., Moritani, K., Kumada, T., Kusukawa, R., 1983. Importance of left atrial function in patients with myocardial infarction. Circulation 67(3), 566–571.

McGuinness, M., Hong, Y., Galletly, D., Larsen, P., 2004. Arnold tongues in human cardiorespiratory systems. Chaos 14(1), 1–6.

Nazir, S.A., Lab, M.J., 1996a. Mechanoelectric feedback and atrial arrhythmias. Cardiovasc. Res. 32, 52–61.

Nazir, S.A., Lab, M.J., 1996b. Mechanoelectric feedback in the atrium of the isolated guinea-pig heart. Cardiovas. Res. 32(1), 112–119.

Ninio, D.M., Murphy, K.J., Howe, P.R., Saint, D.A., 2005. Dietary fish oil protects against stretch-induced vulnerability to atrial fibrillation in a rabbit model. J. Cardiovasc. Electrophysiol. 16(11), 1189–1194.

Nollo, G., Del Greco, M., Ravelli, F., Disertori, M., 1994. Evidence of low- and high-frequency oscillations in human AV interval variability: evaluation with spectral analysis. Am. J. Physiol. 267(4), H1410–H1418.

Page, R.L., Wharton, J.M., Prystowsky, E.N., 1996. Effect of continuous vagal enhancement on concealed conduction and refractoriness within the atrioventricular node. Am. J. Cardiol. 77(4), 260–265.

Ravelli, F., Disertori, M., Cozzi, F., Antolini, R., Allessie, M.A., 1994. Ventricular beats induce variations in cycle length of rapid (type II) atrial flutter in humans. Evidence of leading circle reentry. Circulation 89(5), 2107–2116.

Ravelli, F., Allessie, M., 1997. Effects of atrial dilatation on refractory period and vulnerability to atrial fibrillation in the isolated Langendorff-perfused rabbit heart. Circulation 96(5), 1686–1695.

Ravelli, F., 1998. Atrial flutter cycle length oscillations and role of the autonomic nervous system. Circulation 98(6), 607–608.

Ravelli, F., 2003. Mechano-electric feedback and atrial fibrillation. Progr. Biophys. Mol. Biol. 82(1–3), 137–149.

Rice, J.J., Winslow, R.L., Dekanski, J., McVeigh, E., 1998. Model studies of the role of mechano-sensitive currents in the generation of cardiac arrhythmias. J. Theor. Biol. 190(4), 295–312.

Riemer, T.L., Sobie, E.A., Tung, L., 1998. Stretch-induced changes in arrhythmogenesis and excitability in experimentally based heart cell models. Am. J. Physiol. 275(2), H431–H442.

Riemer, T.L., Tung, L., 2003. Stretch-induced excitation and action potential changes of single cardiac cells. Prog. Biophys. Mol. Biol. 82(1–3), 97–110.

Robotham, J.L., Lixfeld, W., Holland, L., MacGregor, D., Bryan, A.C., Rabson, J., 1978. Effects of respiration on cardiac performance. J. Appl. Physiol. 44(5), 703–709.

Sachs, F., 1991. Mechanical transduction by membrane ion channels: a mini review. Mol. Cell. Biochem. 104(1–2), 57–60.

Sachs, F., 1994. Modeling mechanical-electrical transduction in the heart. In: Mow, V.C., Guliak, F., Tran-Son-Tray, R., Hochmuth, R.M. (Eds.), Cell Mechanics and Cellular Engineering, pp. 308–328. Springer, New York

Shrier, A., Dubarsky, H., Rosengarten, M., Guevara, M.R., Nattel, S., Glass, L., 1987. Prediction of complex atrioventricular conduction rhythms in humans with use of the atrioventricular nodal recovery curve. Circulation 76(6), 1196–1205.

Tavi, P., Han, C., Weckstrom, M., 1998. Mechanisms of stretch-induced changes in [Ca2+]i in rat atrial myocytes: role of increased troponin C affinity and stretch-activated ion channels. Circ. Res. 83(11), 1165–1177.

Tung, L., Zou, S., 1995. Influence of stretch on excitation threshold of single frog ventricular cells. Exp. Physiol. 80(2), 221–235.

Uherka, D.J., Tresser, C., Galeeva, R., Campbell, D.K., 1992. Solvable models for the quasi-periodic transition to chaos. Phys. Lett. A 170(3), 189–194.

Vulliemin, P., Del Bufalo, A., Schlaepfer, J., Fromer, M., Kappenberger, L., 1994. Relation between cycle length, volume, and pressure in type I atrial flutter. Pacing Clin. Electrophysiol. 17(8), 1391–1398.

Waldo, A.L., 2000. Treatment of atrial flutter. Heart 84(2), 227–232.

Warner, M.R., deTarnowsky, J.M., Whitson, C.C., Loeb, J.M., 1986. Beat-by-beat modulation of AV conduction. II. Autonomic neural mechanisms. Am. J. Physiol. 251(6), H1134–H1142.

Warner, M.R., Loeb, J.M., 1986. Beat-by-beat modulation of AV conduction. I. Heart rate and respiratory influences. Am. J. Physiol. 251(6), H1126–H1133.

Waxman, M.B., Yao, L., Cameron, D.A., Kirsh, J.A., 1991. Effects of posture, Valsalva maneuver and respiration on atrial flutter rate: an effect mediated through cardiac volume. J. Am. Coll. Cardiol. 17(7), 1545–1552.

White, E., Le Guennec, J.Y., Nigretto, J.M., Gannier, F., Argibay, J.A., Garnier, D., 1993. The effects of increasing cell length on auxotonic contractions; membrane potential and intracellular calcium transients in single guinea-pig ventricular myocytes. Exp. Physiol. 78(1), 65–78.

Zarse, M., Stellbrink, C., Athanatou, E., Robert, J., Schotten, U., Hanrath, P., 2001. Verapamil prevents stretch-induced shortening of atrial effective refractory period in Langendorff-perfused rabbit heart. J. Cardiovasc. Electrophysiol. 12(1), 85–92.

Zhuang, J., Yamada, K.A., Saffitz, J.E., Kleber, A.G., 2000. Pulsatile stretch remodels cell-to-cell communication in cultured myocytes. Circ. Res. 87(4), 316–322.